Available online at www.sciencedirect.com
ScienceDirect
Tetrahedron
Tetrahedron 63 (2007) 1331–1338

Mixed aggregates of dilithiodiamines with alkyllithiums and lithium enolates

Lawrence M. Pratt,[a,*] R. Mu,[b] Carl Carter[a] and Brittini Woodford[a]

[a] *Department of Chemistry, Fisk University, Nashville, TN 37208, USA*
[b] *Department of Physics, Fisk University, Nashville, TN 37208, USA*

Received 17 October 2006; revised 21 November 2006; accepted 30 November 2006
Available online 19 December 2006

Abstract—The formation of mixed aggregates of *N*,*N*′-dilithiodiamines with alkyllithiums and lithium enolates was investigated. Enolization of 3-pentanone with the dilithium salt of *N*,*N*′-dimethyl-1,3-propanediamine generated both the *E* and *Z* enolates and the *E*/*Z* ratio changed in the presence of a lithium enolate or excess butyllithium. The formation of mixed aggregates was modeled with the B3LYP DFT method and it was found that mixed aggregate formation is energetically favorable. The infrared spectra of dilithio-*N*,*N*′-dimethyl-1,3-propanediamine in the presence of excess butyllithium or lithium enolate are consistent with the formation of mixed aggregates.

---

1. Introduction

Lithium dialkylamides are used extensively in organic synthesis for the formation of enolates. Ketone enolates, such as 3-pentanone, can form *E*/*Z* stereoisomers. Enantioselective synthesis of enolates is a topic of current interest[1–3] and stereoselective synthesis of enolates is a requirement for good enantioselectivity. For example, in a chiral aldol reaction, the *E* enolate will generate one enantiomer and the *Z* enolate will generate the other enantiomer. Enolization selectivity is influenced by several factors, including the lithium dialkylamide structure, solvation, temperature, and mixed aggregate formation.[4–9] Dilithiodiamines were initially investigated as potential bases for ketone enolization with high stereoselectivity because it was anticipated that they would resist mixed aggregate formation due to the formation of energetically favorable intramolecular dimers.[10] The experimental work described in this paper suggests that dilithiodiamines also form mixed aggregates with alkyllithiums and lithium enolates and the results of detailed computational studies are reported. A dilithiodiamine molecule could, in principle form a polycyclic mixed aggregate with a single alkyllithium or lithium enolate molecule, or both ends of the dilithiodiamine could form a simple mixed cyclic dimer with two alkyllithium or lithium enolate molecule. The dilithiodiamines of interest are the lithium salts of *N*,*N*′-dimethylethylenediamine and *N*,*N*′-dimethyl-1,3-propanediamine. The latter compound and its mixed aggregates are soluble in THF and were used in the experimental studies, while the former compound is insoluble and was included in the computational studies to determine the effects of chain length on mixed aggregate formation.

2. Computational and experimental methods

All calculations were performed using *Gaussian 98* or *Gaussian 03*,[11] or NW Chem.[12,13] The gas phase and solution energies reported include gas phase internal energy, thermal corrections to the free energy at 200 and 298 K, and where applicable, solvation terms.

The solvation free energy change of the gas phase organolithium molecule $(\mathrm{RLi})_n$ due to microsolvation by m explicit ethereal solvent ligands E (in this case, dimethyl ether or THF) is calculated by considering the process

$$(\mathrm{RLi})_n + m\mathrm{E} \rightarrow (\mathrm{RLi})_n \cdot m\mathrm{E}. \qquad (1)$$

The microsolvation model assumes that the free energy change accompanying this reaction adequately represents the solvation free energy $\Delta G^0_{\mathrm{solv}}$ of the solute $(\mathrm{RLi})_n$ in the solvent E, so that

$$G^0_T(\mathrm{solute}) = G^0_T(\mathrm{gas}) + \Delta G^0_{\mathrm{solv}}.$$

In other words, the free energy of a 'supermolecule' $(\mathrm{RLi})_n \cdot m\mathrm{E}$ relative to that of m solvent molecules is assumed to yield the free energy of the solvated molecule $(\mathrm{RLi})_n$ in the condensed phase. The gas phase free energies of the relevant species are obtained computationally as

---

* Corresponding author. Tel.: +1 6153298559; e-mail: lpratt@fisk.edu

0040–4020/$ - see front matter © 2006 Elsevier Ltd. All rights reserved.
doi:10.1016/j.tet.2006.11.086

$$G_T^0(\text{gas}) = E_{\text{en}} + \Delta G_T^0, \quad (2)$$

where the terms on the right hand side as well as the procedure used for calculating them are described below. The geometry of each molecule was first optimized using the B3LYP hybrid density functional method[14,15] with the MIDIX basis set,[16] followed by a calculation of vibrational frequencies at the same level of theory. A further refinement of the geometry and energy was done at the B3LYP/6-31+G(d)[17,18] level of theory. This approach has previously generated results that were in good agreement with experimental data for other lithium dialkylamide mixed aggregates[19]. Thus we have:

E_{en}=the electronic energy plus nuclear repulsion of the equilibrium geometry, using B3LYP/6-31+G(d).

E_0^{vib}=unscaled B3LYP/MIDIX vibrational zero point energy.

ΔG_T^0=B3LYP/MIDIX thermal corrections to the free energy for a standard state of 1 atm and specified temperature from the masses. This includes contributions from translational, rotational, and vibrational degrees of freedom.

Calculations for the free energy changes for the 'reactions' (dimerizations, tetramerizations, mixed aggregate formation, etc.) are straightforward using the $G_T^0(\text{gas})$ terms defined in Eq. 2.

Correction terms are needed to convert the gas phase free energies to standard state of a solution, which is taken as 1 mol l^{-1}. The details of these corrections have been previously published.[20] Briefly, a correction is required to convert the standard state of an ideal gas (1 atm) to the standard state of the solution. These corrections amount to 1.1120 kcal/mol at 200 K and 1.8943 kcal/mol at 298 K. These correction terms were included in all solution phase reactions below, i.e., calculations where the microsolvation model was used. Yet another correction is required for proper treatment of the explicit solvent molecules used in microsolvation. The traditional approach is to set the standard state of a pure liquid to be the concentration of the pure liquid itself, which then allows one to drop the concentration of the pure liquid from equilibria expressions (consider the ionic product of water, for example). However, since we have decided to adopt the standard state of 1 mol l^{-1} for all species, the free energy change for the process

$$2\text{RLi}\cdot 2\text{THF} \rightarrow (\text{RLi}\cdot\text{THF})_2 + 2\text{THF} \quad (3)$$

is given by[21]

$$\Delta G^0 = -RT \ln\frac{[(\text{RLi}\cdot\text{THF})_2]}{[\text{RLi}\cdot 2\text{THF}]^2} - 2RT\ln[\text{THF}].$$

The molarity of the THF solvent was calculated to be 13.26 at 200 K and 12.33 at 298 K, from its tabulated density.[22] The corrections due to the second term in the equation above amount to −1.0273 and −1.4883 kcal/mol per THF at 200 and 298 K, respectively. However, for the mixed aggregate formation reactions, in this paper, equal numbers of coordinated THF molecules appeared on each side of the equations, causing these terms to cancel.

All ketone enolizations were performed at −78 °C under a nitrogen atmosphere. The following procedure, adopted from that published by Collum and co-workers,[6] was used to determine the enolization stereoselectivity of the dilithio-*N*,*N*′-dimethyldiaminopropane. Anhydrous THF (2.0 ml) was added to a round bottom flask with 0.8 mmol of *N*,*N*′-dimethyl-1,3-diaminopropane. The temperature was reduced to −40 °C and 1.0 ml (1.6 mmol) of 1.6 M butyllithium in hexane was added. The solution was stirred for 5 min before reducing the temperature to −78 °C. 3-Pentanone was added (1.28 mmol, 0.8 mmol, and 0.4 mmol at 80%, 50%, and 25% conversion of the base, respectively) and the solution stirred for 15 min. Chlorotrimethylsilane (TMSCl, 2.0 mmol) was then added and the solution stirred for an additional 5 min. A 100-μl aliquot of the reaction mixture was dissolved in 1 ml ethyl ether and the *E*/*Z* ratios determined by gas chromatography.

To determine the effects of the dilithiodiamine–butyllithium mixed aggregates, 1.76 mmol of butyllithium was added to the solution of *N*,*N*′-dimethyl-1,3-diaminopropane in THF, resulting in a solution that contained 0.8 mmol of the dilithio-*N*,*N*′-dimethyl-1,3-diaminopropane and a 10% excess of butyllithium. The 3-pentanone was added as before and the *E*/*Z* ratios determined.

The solutions containing dilithio-*N*,*N*′-dimethyl-1,3-diaminopropane with the enolate of cyclohexanone were prepared by adding 1.76 mmol of butyllithium to a solution of 0.8 mmol of *N*,*N*′-dimethyl-1,3-diaminopropane in 2.0 ml THF. Dry cyclohexanone was then added (0.16 mmol) at −78 °C, resulting in a solution of dilithio-*N*,*N*′-dimethyl-1,3-diaminopropane that contained 10 mol % cyclohexanone enolate. 3-Pentanone was added at −78 °C and quenched as before with TMSCl.

The dilithiodiamines for an infrared analysis were prepared from *N*,*N*′-dimethylethylenediamine, *N*,*N*′-dimethyl-1,3-propanediamine, and butyllithium. Butyllithium (1.6 M in hexanes, 2.1 mmol) was added to a solution of 1.0 mmol of the diamine in 8.6 ml THF at −80 °C. The dilithio-*N*,*N*′-dimethylethylenediamine precipitated as a white solid. The THF solution of dilithio-*N*,*N*′-dimethyl-1,3-propanediamine was used for infrared spectroscopic studies. A second solution of dilithio-*N*,*N*′-dimethyl-1,3-propanediamine in THF was prepared with one additional equivalent of butyllithium added for study of mixed aggregate formation. The solution was prepared at −80 °C and allowed to warm to room temperature, where THF is converted to the lithium acetaldehyde enolate over a period of minutes. Infrared spectra were acquired after 20 min and again after 50 min. A separate sample was similarly prepared and allowed to stand overnight to completely convert the butyllithium to the lithium enolate. The spectra were acquired with a polyethylene liquid cell, which is transparent in the spectral region of interest, 200–700 cm^{-1}. One hundred scans were co-added to obtain each spectrum with a 4 cm^{-1} resolution.

3. Results and discussion

3-Pentanone enolization reactions were performed using *N*,*N*′-dilithio-*N*,*N*′-dimethyldiaminopropane (Li_2DMPDA) in THF solution at 195 K, as shown in Scheme 1. Reactions were run at 80%, 50%, and 25% conversion of the lithium amide base. The maximum *E*/*Z* stereoselectivity occurred with a large excess of the dilithiodiamine (25% conversion), which suggests the formation of a dilithiodiamine mixed aggregate with the newly formed enolate. At low percent conversions little of the enolate is present to form a mixed aggregate and enolization occurs via the dilithiodiamine.

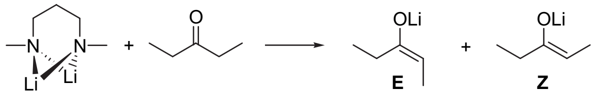

Scheme 1. Ketone enolization by Li_2DMPDA.

To determine the effects of mixed aggregates on the enolization stereoselectivity, the experiment was repeated with 10% excess butyllithium and with 0.1 equiv of the lithium cyclohexanone enolate. The results are shown in Table 1. Both mixed aggregates caused a reduction in stereoselectivity with dilithio-*N*,*N*′-dimethyl-1,3-diaminopropane. From the change in stereoselectivity with percent conversion of the base and from added butyllithium and lithium enolate, we conclude that dilithio-*N*,*N*′-dimethyl-1,3-diaminopropane likely forms mixed aggregates of as yet undetermined structure.

Table 1. Enolization stereoselectivity of 3-pentanone with Li_2DMPDA

Base (% conversion)	*E* (%)	*Z* (%)
Li_2DMPDA (80)	79	21
Li_2DMPDA (50)	79	21
Li_2DMPDA (25)	95	5
Li_2DMPDA+BuLi (80)	65	35
Li_2DMPDA+enolate (80)	71	29

Our previous work found that dilithio-*N*,*N*′-dimethyl-1,3-diaminopropane exists in THF solution exclusively as a bridged cyclic intramolecular dimer and a similar structure was calculated for the THF insoluble dilithio-*N*,*N*′-dimethylethylenediamine (Li_2DMEDA).[10] The ^{6}Li NMR spectrum of ethyllithium in THF at 158 K showed three different aggregates, which were tentatively assigned as monomer, dimer, and tetramer, in analogy to other alkyllithium compounds.[4] Lithium enolates are most often dimeric or tetrameric in ethereal solvents, sometimes in equilibrium with the monomer.[23–27] The system of interest was made computationally tractable with the B3LYP method and a moderately large 6-31+G(d) basis set by use of ethyllithium and the lithium enolate of acetaldehyde for the modeling study. The ethyllithium and lithium enolate dimers were used to calculate the energies of mixed aggregate formation, as shown in Scheme 2. Eq. 4 shows the formation of a polycyclic bridged mixed aggregate containing one mole of the dilithiodiamine and one mole of ethyllithium or lithium enolate. Eq. 5 shows the formation of a mixed dimer with each end of the dilithiodiamine with ethyllithium or lithium enolate, analogous to the formation of mixed dimers of simple lithium dialkylamides.[4,28] The optimized geometries of these gas phase 1:1 mixed aggregates are shown in Figure 1.

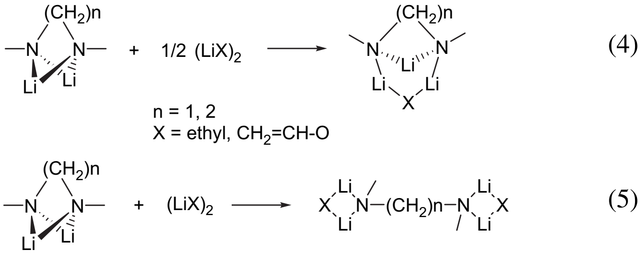

Scheme 2. Gas phase dilithiodiamine mixed aggregate formation.

The calculated free energies of gas phase mixed aggregate formation between the dilithiodiamines and ethyllithium or lithium acetaldehyde enolate are shown in Tables 2 and 3, respectively, for mixed aggregates containing 1 or 2 equiv of ethyllithium or the enolate. The data show that mixed aggregates with ethyllithium and the lithium acetaldehyde enolate form quantitatively. However, in the gas phase, the open mixed trimer depicted in Eq. 5 was not the most stable species. Instead, a bridged structure was energetically favored, in which the two ends of the mixed trimer interacted and formed a more stable complex, shown in Figure 2.

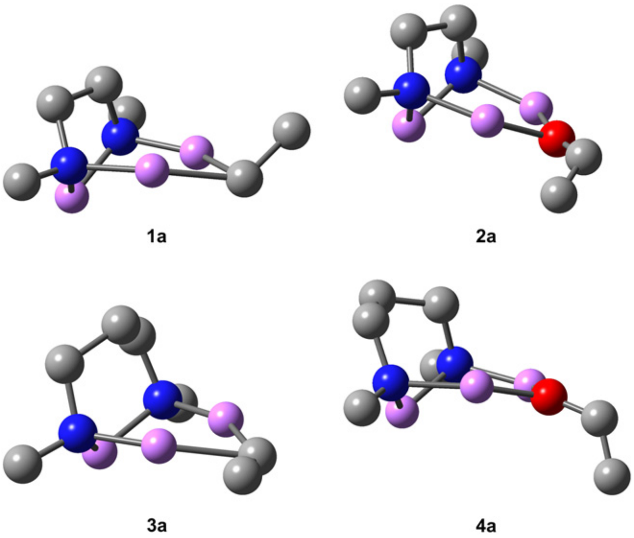

Figure 1. Optimized gas phase geometries of Li_2DMEDA (top) and Li_2DMPDA (bottom) 1:1 mixed aggregates with ethyllithium and lithium acetaldehyde enolate (Eq. 4). Gray: carbon; violet: lithium; blue: nitrogen; red: oxygen. Hydrogens omitted for clarity.

Table 2. Calculated free energies of gas phase 1:1 mixed aggregate formation (kcal/mol)

Str.	Dilithiodiamine	LiX	ΔG^0
200 K			
1a	Li_2DMEDA	EtLi	−15.36
2a	Li_2DMEDA	$LiOCH{=}CH_2$	−15.85
3a	Li_2DMPDA	EtLi	−15.74
4a	Li_2DMPDA	$LiOCH{=}CH_2$	−11.64
298 K			
1a	Li_2DMEDA	EtLi	−13.56
2a	Li_2DMEDA	$LiOCH{=}CH_2$	−14.04
3a	Li_2DMPDA	EtLi	−14.03
4a	Li_2DMPDA	$LiOCH{=}CH_2$	−9.94

Dilithiodiamine+1/2 $(LiX)_2 \rightarrow$ mixed aggregate X=ethyl, O–CH=CH_2.

Table 3. Calculated free energies of gas phase 2:1 mixed aggregate formation (kcal/mol)

Str.	Dilithiodiamine	LiX	ΔG^0
200 K			
5a	Li_2DMEDA	EtLi	−32.9
6a	Li_2DMEDA	$LiOCH{=}CH_2$	−36.6
7a	Li_2DMPDA	EtLi	−27.6
8a	Li_2DMPDA	$LiOCH{=}CH_2$	−30.8
298 K			
5a	Li_2DMEDA	EtLi	−28.1
6a	Li_2DMEDA	$LiOCH{=}CH_2$	−32.0
7a	Li_2DMPDA	EtLi	−22.8
8a	Li_2DMPDA	$LiOCH{=}CH_2$	−26.4

Dilithiodiamine+$(LiX)_2$→mixed aggregate X=ethyl, O–CH=CH$_2$.

The reaction of $Li_2DMEDA\cdot LiX$ (**1a** and **2a**) and $Li_2DMPDA\cdot LiX$ (**3a** and **4a**) with 1/2 equiv of $(LiX)_2$ to form $(Li_2DMEDA)\cdot(LiX)_2$ and $(Li_2DMPDA)\cdot(LiX)_2$, respectively (Eqs. 6 and 7) was shown to occur quantitatively in the gas phase, as shown by the data in Table 4.

$$Li_2DMEDA\cdot LiX + 1/2(LiX)_2 \rightarrow (Li_2DMEDA)\cdot(LiX)_2 \tag{6}$$

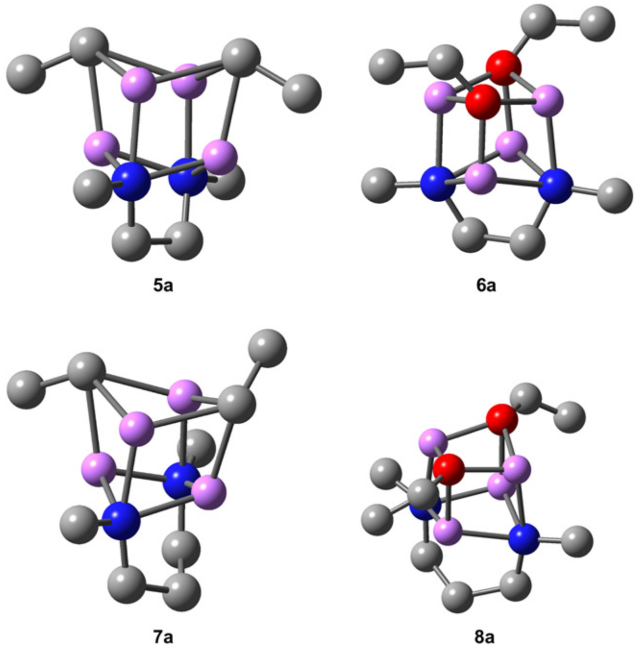
5a 6a 7a 8a

Figure 2. Optimized gas phase geometries of Li_2DMEDA (top) and Li_2DMPDA (bottom) mixed trimers with ethyllithium and lithium acetaldehyde enolate.

Table 4. Calculated free energies of mixed trimer formation from mixed dimer and LiX (kcal/mol) (Eqs. 6 and 7)

Str.	Dilithiodiamine	LiX	ΔG^0
200 K			
5a	Li_2DMEDA	EtLi	−17.5
6a	Li_2DMEDA	$LiOCH{=}CH_2$	−20.8
7a	Li_2DMPDA	EtLi	−11.9
8a	Li_2DMPDA	$LiOCH{=}CH_2$	−19.1
298 K			
5a	Li_2DMEDA	EtLi	−14.6
6a	Li_2DMEDA	$LiOCH{=}CH_2$	−17.9
7a	Li_2DMPDA	EtLi	−8.7
8a	Li_2DMPDA	$LiOCH{=}CH_2$	−16.5

$$Li_2DMPDA\cdot LiX + 1/2(LiX)_2 \rightarrow (Li_2DMPDA)\cdot(LiX)_2 \tag{7}$$

The formation of dimethyl ether and THF solvated mixed aggregates from Li_2DMEDA and Li_2DMPDA is shown in Scheme 3 and the optimized geometries of the mixed aggregates with 1 and 2 equiv of ethyllithium or lithium enolate are shown in Figures 3 and 4, respectively. Solvation was

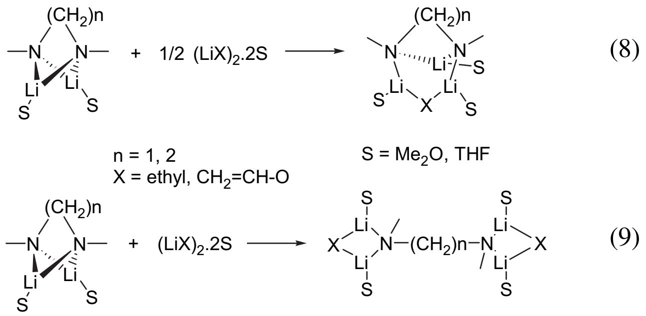

Scheme 3. Solvated dilithiodiamine mixed aggregate formation.

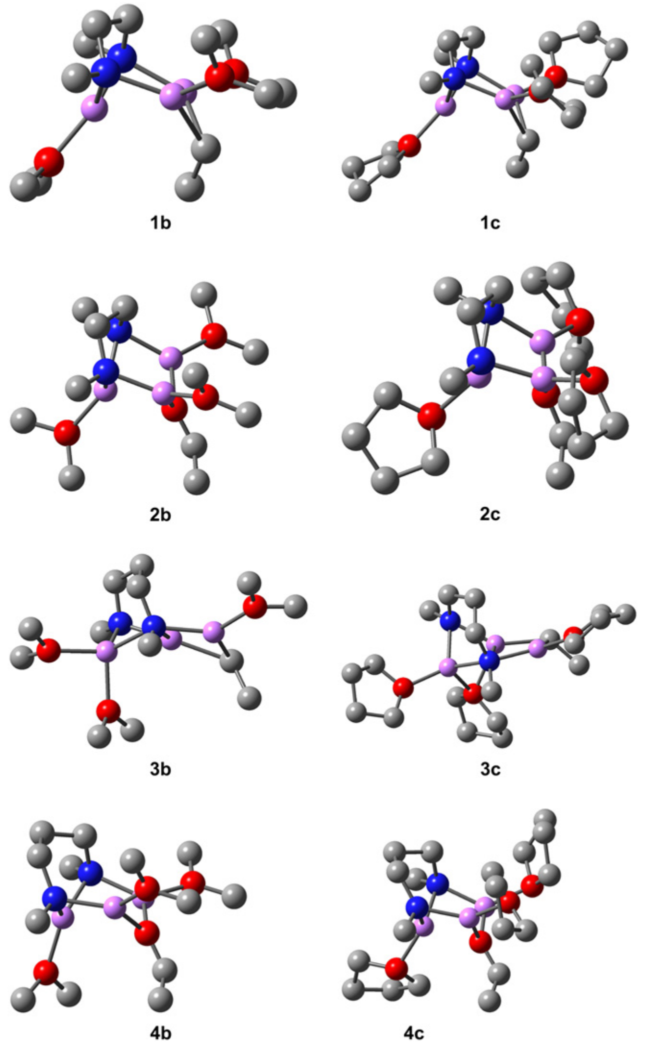
1b 1c 2b 2c 3b 3c 4b 4c

Figure 3. Optimized geometries of Li_2DMEDA and Li_2DMPDA solvated mixed aggregates with 1 equiv of ethyllithium and lithium acetaldehyde enolate. Left column: dimethyl ether solvate; Right column: THF solvate.

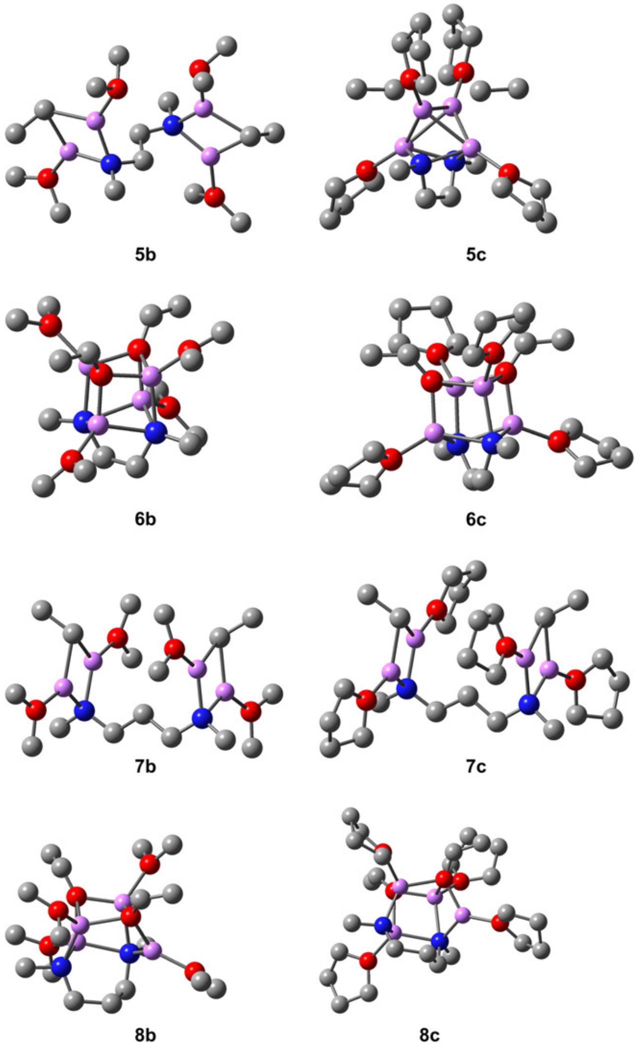

5b 5c

6b 6c

7b 7c

8b 8c

Figure 4. Optimized geometries of Li_2DMEDA and Li_2DMPDA solvated mixed aggregates with 2 equiv of ethyllithium and lithium acetaldehyde enolate. Left column: dimethyl ether solvate; Right column: THF solvate.

modeled using THF to represent the actual solvent of interest, as well as with the computationally cheaper dimethyl ether, which is sometimes used as a model for ethereal solvents. With solvation by either dimethyl ether or THF, the calculations predict Li_2DMEDA to quantitatively form a mixed aggregate with 1 equiv of ethyllithium or lithium acetaldehyde enolate at both 200 and 298 K. Li_2DMPDA was found to be less prone to formation of the analogous mixed aggregates. The dimethyl ether solvated Li_2DMPDA–ethyllithium mixed aggregate was favored by increasing temperatures, while the opposite was true for the enolate mixed aggregate. THF solvation favored the Li_2DMPDA mixed aggregates relative to dimethyl ether, with the mixed aggregate being the predominant species at 200 K and quantitatively formed at 298 K. These results are summarized in Table 5.

The free energies of formation of solvated 2:1 mixed aggregates are shown in Table 6. Unlike the gas phase where only the bridged structures were formed, some open mixed trimers were formed as well, as depicted in Eq. 9. Table 6 shows the free energy for the most energetically favored form of the mixed trimer and the corresponding optimized geometry is shown in Figure 4. In the mixed trimer of Li_2DMEDA with ethyllithium in dimethyl ether, the energy difference between the open and bridged structure was only 0.6 kcal/mol at 200 K and 2.7 kcal/mol at 298 K.

Table 5. Calculated free energies of solvated 1:1 mixed aggregate formation (kcal/mol)

Str.	Dilithiodiamine·2S	LiX·2S	ΔG^0
200 K			
1b	Li_2DMEDA·2eth	EtLi·2eth	−4.94
2b	Li_2DMEDA·2eth	LiOCH=CH_2·2eth	−7.72
1c	Li_2DMEDA·2THF	EtLi·2THF	−4.15
2c	Li_2DMEDA·2THF	LiOCH=CH_2·2THF	−6.70
3b	Li_2DMPDA·2eth	EtLi·2eth	0.46
4b	Li_2DMPDA·2eth	LiOCH=CH_2·2eth	−1.56
3c	Li_2DMPDA·2THF	EtLi·2THF	−2.55
4c	Li_2DMPDA·2THF	LiOCH=CH_2·2THF	−2.28
298 K			
1b	Li_2DMEDA·2eth	EtLi·2eth	−2.85
2b	Li_2DMEDA·2eth	LiOCH=CH_2·2eth	−5.80
1c	Li_2DMEDA·2THF	EtLi·2THF	−2.01
2c	Li_2DMEDA·2THF	LiOCH=CH_2·2THF	−4.63
3b	Li_2DMPDA·2eth	EtLi·2eth	2.90
4b	Li_2DMPDA·2eth	LiOCH=CH_2·2eth	0.523
3c	Li_2DMPDA·2THF	EtLi·2THF	−0.666
4c	Li_2DMPDA·2THF	LiOCH=CH_2·2THF	−0.118

Dilithiodiamine·2S+1/2 $(LiX)_2$·2S→mixed aggregate·3S X=ethyl, O–CH=CH_2; S=Me_2O, THF.

The 2:1 mixed aggregates could potentially be formed from the 1:1 mixed aggregate and excess ethyllithium or lithium enolate, as depicted in Eqs. 10 and 11. The calculated free energies for this process are given in Table 7. These free energies favor the formation of the lithium enolate 2:1 mixed aggregates and all of the free energies show a significant temperature dependence. Solvation by dimethyl ether usually, but not always, generated free energies that were qualitatively similar to solvation by THF. In dimethyl ether, the formation of the Li_2DMPDA mixed trimer with ethyllithium is disfavored, while THF solvation increases the tendency to form that species, although it is not predicted to form quantitatively even at 200 K. Thus, Li_2DMPDA will form primarily the 1:1 mixed dimer with ethyllithium (**3c**) in equilibrium with some of the mixed trimer (**7c**).

$$\begin{aligned}&\mathrm{Li_2DMEDA\cdot LiX\cdot 3S + 1/2(LiX)_2\cdot 2S \rightarrow}\\&\quad\mathrm{(Li_2DMEDA)\cdot(LiX)_2\cdot 4S}\end{aligned} \tag{10}$$

$$\begin{aligned}&\mathrm{Li_2DMPDA\cdot LiX\cdot 3S + 1/2(LiX)_2\cdot 2S \rightarrow}\\&\quad\mathrm{(Li_2DMPDA)\cdot(LiX)_2\cdot 4S}\end{aligned} \tag{11}$$

The infrared spectra of Li_2DMPDA and its mixed aggregates are shown in Figure 5. Spectrum (a) is for a 0.1 M solution of Li_2DMPDA in THF and the broad peak in the 350–650 cm^{-1} region is consistent with the calculated infrared frequencies of the THF-tetrasolvated bridged Li_2DMPDA structure. Spectra (b), (c), and (d) are of the Li_2DMPDA solution with an additional 2 mmol of butyllithium added, after aging the solution at room temperature for 20 min, 50 min, and overnight. The aging of the solution allowed deprotonation

Table 6. Calculated free energies of solvated 2:1 mixed aggregate formation (kcal/mol)

Str.	Dilithiodiamine·2S	LiX·2S	ΔG^0	Open/bridged
200 K				
5b	$\mathrm{Li_2DMEDA}$·2eth	EtLi·2eth	−2.62	Open
6b	$\mathrm{Li_2DMEDA}$·2eth	$\mathrm{LiOCH{=}CH_2}$·2eth	−13.6	Bridged
5c	$\mathrm{Li_2DMEDA}$·2THF	EtLi·2THF	−8.78	Bridged
6c	$\mathrm{Li_2DMEDA}$·2THF	$\mathrm{LiOCH{=}CH_2}$·2THF	−12.6	Bridged
7b	$\mathrm{Li_2DMPDA}$·2eth	EtLi·2eth	5.00	Open
8b	$\mathrm{Li_2DMPDA}$·2eth	$\mathrm{LiOCH{=}CH_2}$·2eth	−7.33	Bridged
7c	$\mathrm{Li_2DMPDA}$·2THF	EtLi·2THF	0.541	Open
8c	$\mathrm{Li_2DMPDA}$·2THF	$\mathrm{LiOCH{=}CH_2}$·2THF	−8.24	Bridged
298 K				
5b	$\mathrm{Li_2DMEDA}$·2eth	EtLi·2eth	0.497	Open
6b	$\mathrm{Li_2DMEDA}$·2eth	$\mathrm{LiOCH{=}CH_2}$·2eth	−8.84	Bridged
5c	$\mathrm{Li_2DMEDA}$·2THF	EtLi·2THF	−5.47	Bridged
6c	$\mathrm{Li_2DMEDA}$·2THF	$\mathrm{LiOCH{=}CH_2}$·2THF	−7.65	Bridged
7b	$\mathrm{Li_2DMPDA}$·2eth	EtLi·2eth	9.83	Open
8b	$\mathrm{Li_2DMPDA}$·2eth	$\mathrm{LiOCH{=}CH_2}$·2eth	−2.85	Bridged
7c	$\mathrm{Li_2DMPDA}$·2THF	EtLi·2THF	3.81	Open
8c	$\mathrm{Li_2DMPDA}$·2THF	$\mathrm{LiOCH{=}CH_2}$·2THF	−3.77	Bridged

Dilithiodiamine·2S+$\mathrm{(LiX)_2}$·2S→mixed aggregate·4S X=ethyl, $\mathrm{O{-}CH{=}CH_2}$; S=$\mathrm{Me_2O}$, THF.

of THF, followed by a retro-cycloaddition, to form the lithium acetaldehyde enolate, on a timescale of minutes at room temperature. After 20 min, new peaks had appeared at about 290 and 675 $\mathrm{cm^{-1}}$. In addition, there were smaller peaks in the 400–600 $\mathrm{cm^{-1}}$ region. After 50 min the broad peak beginning at about 410 $\mathrm{cm^{-1}}$ and two smaller peaks between 525 and 600 $\mathrm{cm^{-1}}$ had grown larger as butyllithium was converted to lithium enolate and appear as strong peaks in spectrum (d).

The calculated vibrational frequencies indicated that the strong vibration at about 675 $\mathrm{cm^{-1}}$ could come from the open form of the $\mathrm{Li_2DMPDA}$ 2:1 mixed aggregates of both butyllithium or the lithium enolate. It was assumed that the calculated mixed aggregates of ethyllithium will have similar vibrational frequencies in this region to the butyllithium mixed aggregates used in the experimental studies. A smaller contribution to this peak may come from the bridged form of the lithium enolate mixed aggregate.

The observed vibrational frequencies in the 400–500 $\mathrm{cm^{-1}}$ region are consistent with the calculated frequencies of several differently mixed aggregates, including the bridged and open forms of the ethyllithium and lithium enolate 2:1 mixed trimers. The large number of calculated frequencies in this region precludes a definite assignment of these peaks. The vibrations in the 500–600 $\mathrm{cm^{-1}}$ region are also difficult to assign quantitatively, but are consistent with strong calculated frequencies in that region from the open and bridged 2:1 lithium enolate mixed trimers, as well as the 1:1 mixed dimer. The peak at about 290 $\mathrm{cm^{-1}}$ does not correlate with any strong calculated vibrations and its origin remains a mystery. Possible contributions include other solvation states of the various aggregates, as a prior investigation demonstrated a strong correlation between solvation and the vibrational frequencies.[10]

4. Conclusions

$\mathrm{Li_2DMEDA}$ and $\mathrm{Li_2DMPDA}$ form mixed aggregates with butyllithium and lithium enolates. Mixed aggregates of both the lithium enolate and alkyllithium reduce the stereoselectivity of 3-pentanone enolization by $\mathrm{Li_2DMPDA}$,

Table 7. Calculated free energies of mixed trimer formation from mixed dimer and LiX (kcal/mol) (Eqs. 10 and 11)

Str.	Dilithiodiamine·2S	LiX·2S	ΔG^0	Open/bridged
200 K				
5b	$\mathrm{Li_2DMEDA}$·2eth	EtLi·2eth	2.32	Open
6b	$\mathrm{Li_2DMEDA}$·2eth	$\mathrm{LiOCH{=}CH_2}$·2eth	−5.93	Bridged
5c	$\mathrm{Li_2DMEDA}$·2THF	EtLi·2THF	−4.62	Bridged
6c	$\mathrm{Li_2DMEDA}$·2THF	$\mathrm{LiOCH{=}CH_2}$·2THF	−5.87	Bridged
7b	$\mathrm{Li_2DMPDA}$·2eth	EtLi·2eth	4.52	Open
8b	$\mathrm{Li_2DMPDA}$·2eth	$\mathrm{LiOCH{=}CH_2}$·2eth	−5.77	Bridged
7c	$\mathrm{Li_2DMPDA}$·2THF	EtLi·2THF	3.09	Open
8c	$\mathrm{Li_2DMPDA}$·2THF	$\mathrm{LiOCH{=}CH_2}$·2THF	−5.95	Bridged
298 K				
5b	$\mathrm{Li_2DMEDA}$·2eth	EtLi·2eth	3.35	Open
6b	$\mathrm{Li_2DMEDA}$·2eth	$\mathrm{LiOCH{=}CH_2}$·2eth	−3.03	Bridged
5c	$\mathrm{Li_2DMEDA}$·2THF	EtLi·2THF	−3.45	Bridged
6c	$\mathrm{Li_2DMEDA}$·2THF	$\mathrm{LiOCH{=}CH_2}$·2THF	−3.02	Bridged
7b	$\mathrm{Li_2DMPDA}$·2eth	EtLi·2eth	6.92	Open
8b	$\mathrm{Li_2DMPDA}$·2eth	$\mathrm{LiOCH{=}CH_2}$·2eth	−3.38	Bridged
7c	$\mathrm{Li_2DMPDA}$·2THF	EtLi·2THF	4.48	Open
8c	$\mathrm{Li_2DMPDA}$·2THF	$\mathrm{LiOCH{=}CH_2}$·2THF	−3.65	Bridged

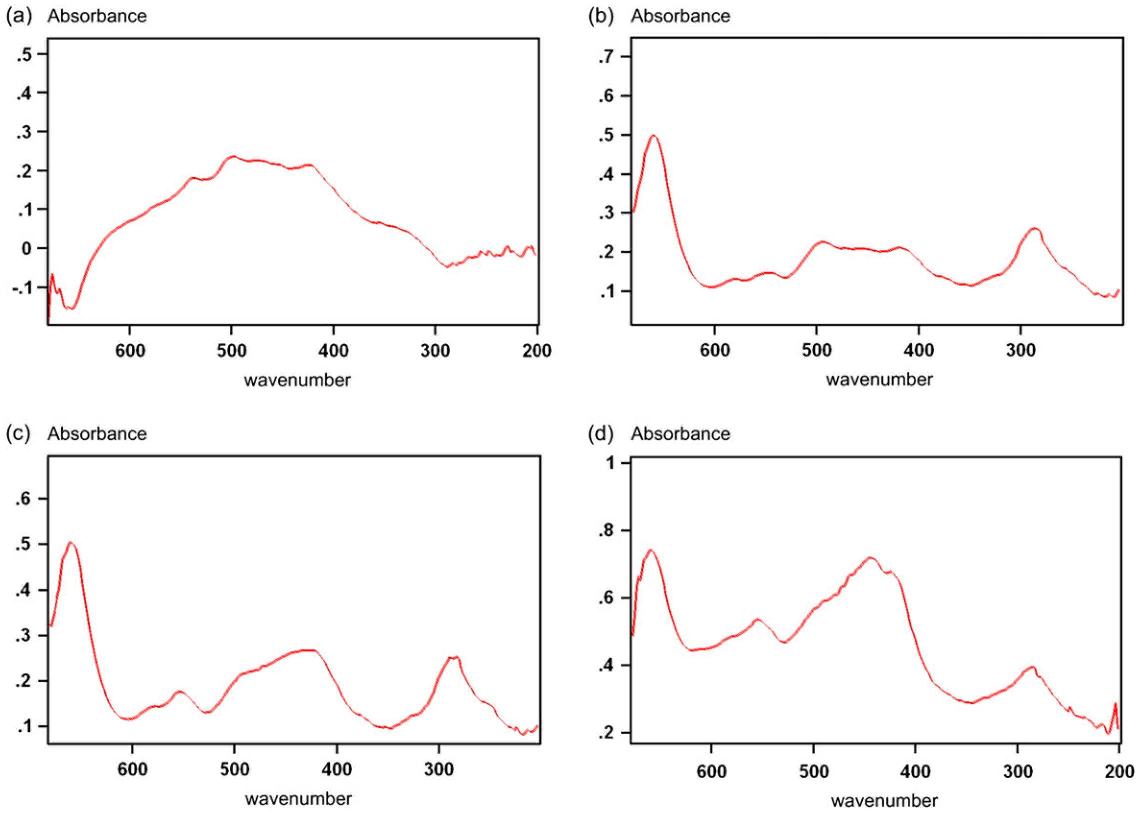

Figure 5. Infrared spectra of Li_2DMPDA and its mixed aggregates. (a) Li_2DMPDA 1.0 M in THF; (b) 2 mmol butyllithium added, solution aged for 20 min; (c) solution aged for 50 min; and (d) solution aged overnight.

while Li_2DMEDA and its mixed aggregates are THF insoluble and thus are not useful for stereoselective enolization reactions. However, these mixed aggregates may prove useful for other types of lithium dialkylamide reactions. DFT calculations show that for the lithium enolate–Li_2DMPDA system, the bridged mixed trimer is the dominant species in THF. A bridged mixed dimer is the dominantly mixed aggregate of ethyllithium. In most cases, solvation by the less expensive dimethyl ether predicted mixed aggregates qualitatively similar to those formed in THF. The infrared spectra are consistent with Li_2DMPDA mixed aggregate formation.

Acknowledgements

This work was supported in part by the Petroleum Research Fund grant #36660-B1, NIH-MBRS grant #S06-GM62813-01, NSF grant #CHE-0139076, and the NSF-RSEC grant #NSF-CHE-0113894. Computer time was provided by the Environmental Molecular Sciences Laboratory (EMSL) at the Pacific Northwest Laboratory. The authors also acknowledge the assistance of Donald G. Truhlar and Cristopher J. Cramer at the University of Minnesota.

Supplementary data

Tables of optimized geometries of dilithiodiamines, lithium enolate, and ethyllithium dimers and all mixed aggregates. Also included are B3LYP/MIDIX calculated vibrational frequencies in the range 200–700 cm^{-1}. Supplementary data associated with this article can be found in the online version, at doi:10.1016/j.tet.2006.11.086.

References and notes

1. Jiang, M.; Zhu, S.-F.; Yang, Y.; Gong, L.-Z.; Zhou, X.-G.; Zhou, Q.-L. *Tetrahedron: Asymmetry* **2006**, *17*, 384.
2. Iskishima, H.; Sekiguchi, Y.; Ichikawa, Y.; Kotsuki, H. *Tetrahedron* **2006**, *62*, 311.
3. Wu, g.; Huang, M. *Chem. Rev.* **2006**, *106*, 2596.
4. Pratt, L. M.; Newman, A.; St. Cyr, J.; Johnson, H.; Miles, B.; Lattier, A.; Austin, E.; Henderson, S.; Hershey, B.; Lin, M.; Balamraju, Y.; Sammonds, L.; Cheramie, J.; Karnes, J.; Hymel, E.; Woodford, B.; Carter, C. *J. Org. Chem.* **2003**, *68*, 6387.
5. Balamraju, Y.; Sharp, C. D.; Gammill, W.; Manuel, N.; Pratt, L. M. *Tetrahedron* **1998**, *54*, 7357.
6. Hall, P. L.; Gilchrist, J. H.; Collum, D. B. *J. Am. Chem. Soc.* **1991**, *113*, 9571.
7. Hall, P. L.; Gilchrist, J. H.; Harrison, A. T.; Fuller, D. J.; Collum, D. B. *J. Am. Chem. Soc.* **1991**, *113*, 9575.
8. Sakuma, K.; Gilchrist, J. H.; Romesberg, F. E.; Cajthami, C. E.; Collum, D. B. *Tetrahedron Lett.* **1993**, *34*, 5213.
9. Corey, E. J.; Gross, A. W. *Tetrahedron Lett.* **1984**, *25*, 495.
10. Pratt, L. M.; Mu, R. *J. Org. Chem.* **2004**, *69*, 7519.
11. Frisch, M. J.; Trucks, G. W.; Schlegel, H. B.; Scuseria, G. E.; Robb, M. A.; Cheeseman, J. R.; Montgomery, J. A., Jr.; Vreven, T.; Kudin, K. N.; Burant, J. C.; Millam, J. M.; Iyengar, S. S.; Tomasi, J.; Barone, V.; Mennucci, B.;

Cossi, M.; Scalmani, G.; Rega, N.; Petersson, G. A.; Nakatsuji, H.; Hada, M.; Ehara, M.; Toyota, K.; Fukuda, R.; Hasegawa, J.; Ishida, M.; Nakajima, T.; Honda, Y.; Kitao, O.; Nakai, H.; Klene, M.; Li, X.; Knox, J. E.; Hratchian, H. P.; Cross, J. B.; Adamo, C.; Jaramillo, J.; Gomperts, R.; Stratmann, R. E.; Yazyev, O.; Austin, A. J.; Cammi, R.; Pomelli, C.; Ochterski, J. W.; Ayala, P. Y.; Morokuma, K.; Voth, G. A.; Salvador, P.; Dannenberg, J. J.; Zakrzewski, V. G.; Dapprich, S.; Daniels, A. D.; Strain, M. C.; Farkas, O.; Malick, D. K.; Rabuck, A. D.; Raghavachari, K.; Foresman, J. B.; Ortiz, J. V.; Cui, Q.; Baboul, A. G.; Clifford, S.; Cioslowski, J.; Stefanov, B. B.; Liu, G.; Liashenko, A.; Piskortz, P.; Komaromi, I.; Martin, R. L.; Fox, D. J.; Keith, T.; Al-Laham, M. A.; Peng, C. Y.; Nanayakkara, A.; Challacombe, M.; Gill, P. M. W.; Johnson, B.; Chem, W.; Wong, M. W.; Gonzalez, C.; Pople, J. A. *Gaussian 03, Revision A.1*; Gaussian: Pittsburgh, PA, 2003.

12. Straatsma, T. P.; Aprà, E.; Windus, T. L.; Bylaska, E. J.; de Jong, W.; Hirata, S.; Valiev, M.; Hackler, M. T.; Pollack, L.; Harrison, R. J.; Dupuis, M.; Smith, D. M. A.; Nieplocha, J.; Tipparaju, V.; Krishnan, M.; Auer, A. A.; Brown, E.; Cisneros, G.; Fann, G. I.; Fruchtl, H.; Garza, J.; Hirao, K.; Kendall, R.; Nichols, J.; Tsemekhman, K.; Wolinski, K.; Anchell, J.; Bernholdt, D.; Borowski, P.; Clark, T.; Clerc, D.; Dachsel, H.; Deegan, M.; Dyall, K.; Elwood, D.; Glendening, E.; Gutowski, M.; Hess, A.; Jaffe, J.; Johnson, B.; Ju, J.; Kobayashi, R.; Kutteh, R.; Lin, Z.; Littlefield, R.; Long, X.; Meng, B.; Nakajima, T.; Niu, S.; Rosing, M.; Sandrone, G.; Stave, M.; Taylor, H.; Thomas, G.; van Lenthe, J.; Wong, A.; Zhang, Z. *NW Chem, A Computational Chemistry Package for Parallel Computers, Version 4.6*; Pacific Northwest National Laboratory: Richland, Washington, DC, 2004.
13. Kendall, R. A.; Aprà, E.; Bernholdt, D. E.; Bylaska, E. J.; Dupuis, M.; Fann, G. I.; Harrison, R. J.; Ju, J.; Nichols, J. A.; Nieplocha, J.; Straatsma, T. P.; Windus, T. L.; Wong, A. T. *Comput. Phys. Commun.* **2000**, *128*, 260.
14. Becke, A. D. *J. Chem. Phys.* **1993**, *98*, 5648.
15. Stephens, P. J.; Devlin, F. J.; Chabalowski, G. C.; Frisch, M. J. *J. Phys. Chem.* **1994**, *98*, 11623.
16. Clark, T.; Chandresekhar, J.; Schleyer, P. v. R. *J. Comput. Chem.* **1983**, *4*, 294.
17. Lynch, B. J.; Zhao, Y.; Truhlar, D. G. *J. Phys. Chem.* **2003**, *107*, 1384.
18. Thompson, J. D.; Winget, P.; Truhlar, D. G. *Phys. Chem. Commun.* **2001**, *16*, 1.
19. Pratt, L. M. *Bull. Chem. Soc. Jpn.* **2005**, *78*, 890.
20. Pratt, L. M.; Merry, S.; Nguyen, S. C.; Quan, P.; Thanh, B. T. *Tetrahedron* **2006**, *62*, 10821.
21. Thompson, J. D.; Cramer, C. J.; Truhlar, D. G. *J. Chem. Phys.* **2003**, *119*, 1661.
22. Govender, U. P.; Letcher, T. M.; Garg, S. K.; Ahluwalia, J. C. *J. Chem. Eng. Data* **1996**, *41*, 147.
23. Jackman, L. M.; Lange, B. C. *J. Am. Chem. Soc.* **1981**, *103*, 4494.
24. Abbotto, A.; Streitwieser, A. *J. Am. Chem. Soc.* **1995**, *117*, 6358.
25. Abbotto, A.; Shun-Wang, S.; Streitwieser, A.; Kilway, K. V. *J. Am. Chem. Soc.* **1998**, *120*, 10807.
26. Streitwieser, A.; Wang, D. Z.-R. *J. Am. Chem. Soc.* **1999**, *121*, 6213.
27. Wang, D. Z.-R.; Kim, Y.-J.; Streitwieser, A. *J. Am. Chem. Soc.* **2000**, *122*, 10754.
28. Pratt, L. M.; Streitwieser, A. *J. Org. Chem.* **2003**, *68*, 2830.